



Impact of lockdown measures to combat Covid-19 on air quality over western Europe



Laurent Menut^{a,*}, Bertrand Bessagnet^{a,b}, Guillaume Siour^c, Sylvain Mailler^a, Romain Pennel^a, Arineh Cholakian^a

^a Laboratoire de Météorologie Dynamique (LMD), Ecole Polytechnique, IPSL Research University, Ecole Normale Supérieure, Université Paris-Saclay, Sorbonne Universités, UPMC Univ Paris 06, CNRS, Route de Saclay, 91128 Palaiseau, France

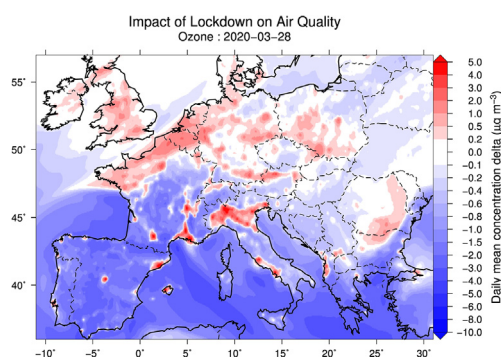
^b Now at Citepa, Technical Reference Center for Air Pollution and Climate Change, 42, rue de Paradis, 75010 Paris, France

^c Laboratoire Interuniversitaire des Systèmes Atmosphériques (LISA), UMR CNRS 7583, Université Paris Est Créteil et Université de Paris, Institut Pierre Simon Laplace, Créteil, France

HIGHLIGHTS

- Air pollution modelling
- COVID19 epidemic
- Regional modelling
- Anthropogenic emissions scenario
- Impact of emissions reduction

GRAPHICAL ABSTRACT



ARTICLE INFO

Article history:

Received 10 May 2020

Received in revised form 19 June 2020

Accepted 20 June 2020

Available online xxxx

Keywords:

COVID-19

Lockdown

Chemistry-transport modelling

Emissions scenario

CHIMERE

ABSTRACT

Recent studies based on observations have shown the impact of lockdown measures taken in various European countries to contain the Covid-19 pandemic on air quality. However, these studies are often limited to compare situations without and with lockdown measures, which correspond to different time periods and then under different meteorological conditions. We propose a modelling study with the WRF-CHIMERE modelling suite for March 2020, an approach allowing to compare atmospheric composition with and without lockdown measures without the biases of meteorological conditions. This study shows that the lockdown effect on atmospheric composition, in particular through massive traffic reductions, has been important for several short-lived atmospheric trace species, with a large reduction in NO₂ concentrations, a lower reduction in Particulate Matter (PM) concentrations and a mitigated effect on ozone concentrations due to non-linear chemical effects.

© 2020 The Authors. Published by Elsevier B.V. This is an open access article under the CC BY-NC-ND license (<http://creativecommons.org/licenses/by-nc-nd/4.0/>).

1. Introduction

The Covid-19 pandemic outbreak has largely impacted the whole world with impressive sanitary and economic consequences, (Muhammad et al., 2020). One of the consequences is the establishment

of unprecedented lockdown and restrictions measures in a large number of countries. Travel restrictions and the obligation to remain in our residence homes to limit the spread of the virus are expected to largely modify anthropogenic emissions of pollutants, both in terms of emitted mass and time variations. The change of these emissions is expected to modify surface pollutants concentrations observed in Europe. This has been observed since the beginning of the lockdown in particular through the analysis of measurements from air quality monitoring

* Corresponding author.

E-mail address: menut@lmd.polytechnique.fr (L. Menut).

networks and satellites. In January 2020, and in China, where the pandemic starts, Shi and Brasseur (2020) analyzed surface measurements data and show that the lockdown (and the probable variability of meteorology) reduced by 35% and 60% the surface concentrations of PM_{2.5} and NO₂, respectively. For ozone, we found an increase by a factor 1.5. Using surface measurements, on the Barcelona region (Spain), (Tobias et al., 2020) noted a decrease of −45 to −51% for BC (Black Carbon) and NO₂, −28 to −31% for PM₁₀. They also noted an increase for ozone, +33% to +57% for the daily maxima. Focusing on Spain, Petetin et al. (2020) are using surface observations and machine learning to retrieve the usual NO₂ if lockdown conditions would have not been present. They found on average that the lockdown measures are responsible of 50% of the observed NO₂ decrease. Similar results with sometimes an increase of Ozone concentrations are observed in Milan as reported by Collivignarelli et al. (2020). The impact of the virus was also evaluated by using satellite data such as NO₂ retrievals using the TROPOMI and OMI observations in Bauwens et al. (2020). They showed a significant decrease of −20% to −38% in western Europe of NO₂ tropospheric column concentrations.

However, these observed changes correspond to a budget and integrate several possible factors: (i) a different meteorology from previous comparison period or years, (ii) a year to year decrease in anthropogenic emissions in Western Europe and (iii) the current lockdown measures to combat the Covid-19 virus. In order to calculate the relative part due to lockdown measures only, a modelling system must be used to assess a change of anthropogenic emissions. For this purpose, a scenario of anthropogenic emissions have been developed and tested taking into account emission reductions calculated by country and activity sectors. Studies of this type are beginning to be published. For example, (Sharma et al., 2020) in India showed a decrease in PM_{2.5} and PM₁₀ concentrations up to respectively 43 and 31% and an increase of 17% ozone concentrations from 16 March to 14 April 2020 confirming the analysis based on observed datasets.

For this study, the WRF-CHIMERE modelling system was used on a spatial domain covering Western Europe. An emission scenario was set up using Apple public data (<https://www.apple.com/covid19/mobility>). Two simulations were carried out for the month of March 2020, (i) a reference simulation with 'business as usual' emissions and (ii) the scenario reflecting the 'reality' of emission changes due to lockdown measures. The difference between both simulations makes it possible to quantify the impact of the consequences of lockdown measures. The modelling system used is presented in Section 2.1 and the emissions scenario in Section 2.2. The results are presented and discussed in Section 3. Conclusions are presented in Section 4.

2. Method

2.1. The modelling system

The WRF 3.7.1, (Skamarock et al., 2007), and CHIMERE models v2017r4 (Mailler et al., 2017) are used to simulate the hourly concentrations of numerous pollutants over Western Europe. This modelling system was recently used for example in (Menut et al., 2019), (Bessagnet et al., 2020).

The WRF model is forced by the NCEP/GFS (Kalnay et al. (1996)) global fields using spectral nudging, (Von Storch et al., 2000). This allows WRF to create its own structures within the boundary layer but being sure it follows the large scale meteorological fields. CHIMERE has been developed since 1997 and used for forecast and analysis since then, Vautard et al. (2000), Honoré et al. (2008), Rouïl et al. (2009), Menut and Bessagnet (2010), Menut et al. (2015b), Maréchal et al. (2015). The model has been compared frequently to various kind of measurements (surface stations, soundings, airborne, satellite), including meteorology and chemistry, Menut et al. (2000), Menut et al. (2005a), Pirovano et al. (2007), Menut et al. (2015a), Bessagnet et al. (2016), Vivanco et al. (2017). The chemical mechanisms for gaseous

species and aerosols are updated following the current knowledge in the field, Bessagnet et al. (2010), Mailler et al. (2016), Couvidat et al. (2018), Cholakian et al. (2018). Regularly, a new version is proposed to the users and detailed in publication, such as in Menut et al. (2013) and Mailler et al. (2017) for the two last versions. If ozone and nitrogen oxides are model species representing exactly the real species, particulate matter (PM) are model species composed of several aerosols. In this study, PM_{2.5} and PM₁₀ represent the concentration of aerosols with mean mass median diameter lower than 2.5 and 10 μm respectively. They are composed of sulphate, nitrate, ammonium, primary organic matter (POM) and elemental carbon (EC), secondary organic aerosols (SOA), sea salt and mineral dust. These aerosols are represented by a diameter size distribution ranging from 10 nm to 40 μm, with 10 bins. Even though the study is focused on anthropogenic emissions, CHIMERE also includes natural emissions to calculate realistic concentrations of all considered gaseous and aerosols species. Biogenic emissions are calculated with the online MEGAN model, Guenther et al. (2006), mineral dust emissions are calculated using the scheme of Alfaro and Gomes (2001) modified after Menut et al. (2005b), sea-salt emissions with the Monahan (1986) scheme.

The simulation period covers the whole month of March 2020, with a spin-up 10-days period in February, from 20 to 29 February. Two horizontal domains are defined: MED60 and EUR20 with respectively Δx=60 km and Δx=20 km as horizontal resolution. The Fig. 1 represents the urban fraction of each cell on these domains. The MED60 domain is defined to take into account all anthropogenic and natural emissions around the Western Europe. A large part of North Africa up to the Middle East is also covered to account for possible long range transport of gaseous species and particles. EUR20 is designed for the present analysis and used the simulation of MED60 as hourly boundary conditions. Only the simulation over EUR20 will be analyzed in this study.

For domain EUR20 domain, two simulations are performed, (i) a reference simulation (REF) without lockdown measures using classical emissions and (ii) a simulation (CVD) taking into account an estimate of lockdown measures on pollutant emissions. Results are presented

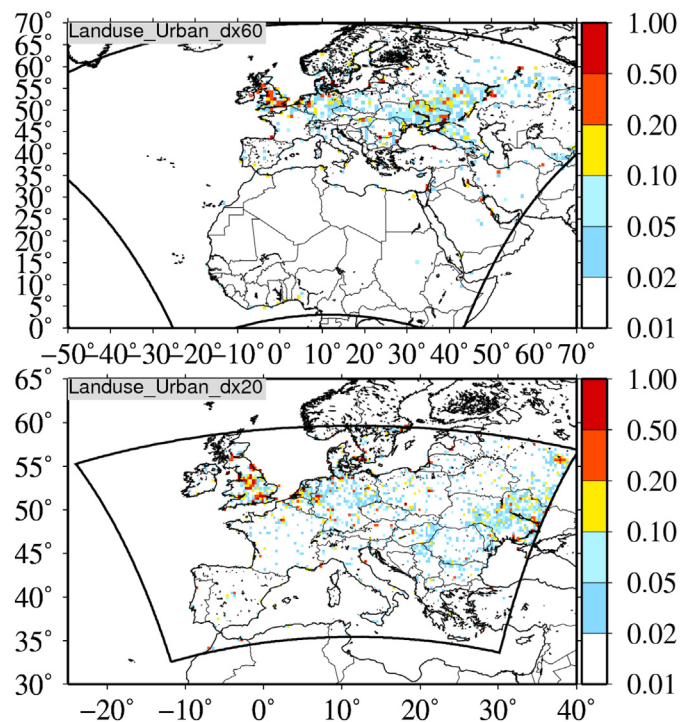


Fig. 1. The two simulation domains used in this study. Colors indicate the percentage of 'urban' landuse in the grid cell. (For interpretation of the references to color in this figure legend, the reader is referred to the web version of this article.)

for the month of March 2020. They represent the impact of anthropogenic emission reductions due to containment measures and their successive implementation in most European countries. In this study, the MED60 simulation is performed one time with classical emissions with no lockdown impacts and used to drive the two simulations over the EUR20 domain: REF and CVD. The consequence of this choice is two-fold: (i) there is no impact of very long range transport of lockdown measures coming from areas outside the EUR20 domain, and (ii) possible recirculation at the border of the EUR20 are not taken into account.

Even if all results are not perfect, with biases, uncertainties, we can be confident with two important points for this study: (i) the model has the right orders of magnitude and space-time variability for all chemical species. This means that the transport is correct between sources and measurements, and also that the chemistry and deposition are correct throughout the transport of the species. (ii) as the model was validated in many different circumstances, it is known to react logically to an increase or decrease in emissions. One can therefore be confident in the results of the emissions scenarios in terms of the sign and magnitude of the calculated differences.

2.2. The anthropogenic emissions scenario

The anthropogenic emissions for the MED60 domain are from the CAMS database (available at <https://eccad3.sedoo.fr/#CAMS-GLOB-ANT>, Granier et al. (2019)) for the available year 2019. For the EUR20 domain emissions are from the EMEP (European Monitoring and Evaluation Programme, (Mareckova et al., 2019)) database released in 2019 and available for year 2017. This dataset corresponds to the most state-of-the-art and up-to-date dataset for anthropogenic emissions in Europe. For the reference simulation, REF, this dataset was used with the EMISURF pre-processing program, developed by the same group as the CHIMERE model. This program is able to read many different format of raw anthropogenic emissions to prepare files with data projected on the CHIMERE grid, with one fields per week day for a given month and for the chemical species used for the simulation. Many details about this preparation program are presented in Menut et al. (2012) and Mailler et al. (2017).

Estimating emissions during the lockdown period, the CVD simulation, is the most challenging part of this study. Only anthropogenic emissions for EUR20 are changed to account for lockdown measures. The Apple company has provided a dataset as an estimate of “driving”, “transit” and “cycling” daily activities from 13 January 2020 for tens of countries in the world. This dataset is a compilation of anonymized and aggregated data retrieve from mobile Apple devices when users search map information.

Most of European countries are covered by this dataset. We use the “driving” dataset to estimate the reduction or increase of traffic activity base on a reference state. Because emission data in CHIMERE already account for a weekly factor to distinguish emissions from Monday to Sunday we have normalized for each available country the Apple dataset by dividing by the activity dataset of a “normal” day of week before the lockdown measures. We have selected the 7 days from Monday 13 to 20 January 2020 as the reference period for this weekdays adjustment process. The change of road traffic emissions in March 2020 is then calculated based on a change of “driving” activity from Apple data and is applied to the road traffic sector (SNAP 7) for all pollutants. During the lockdown period reduction from -50 to -80% are observed for many European countries, see Fig. 2. This daily reduction factor for the road traffic is called f_7 , a positive value stands for a reduction. Outside the lockdown period this factor can be slightly positive or negative as it reflects the reality of day to day traffic variations but during the lockdown it remains largely negative. For instance in Spain are supposed to be 10 to 20% in the beginning of March compared to ‘business-as-usual’ emissions, this characteristics is difficult to explain and could be due to unusual emissions due to pre-lockdown activities (e.g. change of residence homes). It is noteworthy that in our study we do not distinguish

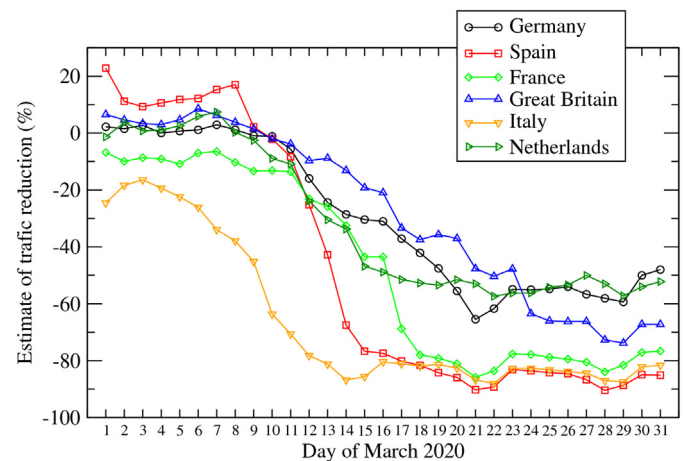


Fig. 2. Traffic reduction for several countries in Western Europe. This factor is normalized to reference days in January 2020.

regional difference of lockdown measures in countries; for instance in Italy, the north part of the country adopted restriction measures earlier compared to the rest of the country.

For the other SNAP sectors (Selected Nomenclature for Air Pollution), we use the factor f_7 to scale the emission change for the other sectors applied to all pollutants. For the industrial sectors (SNAP 3, 4, 5 and 6) a factor $f_7/2$ is applied. We decided to not apply any reduction factors for the Energy sector (SNAP 1) since any relevant data were not available at the beginning of this study. The agricultural sector (SNAP 10) and the waste sector (SNAP 9) are supposed to be not affected by the lockdown measures. For the off-road sector (SNAP 8) a reduction of $f_7/2$ is applied mainly to account for a reduction of the aviation activity even if this sector at the national level is not dominant (e.g. less than 2% of NO_2 emissions during the Landing-Take-Off aircraft operations of total NO_2 emissions in France).

Conversely, as people are asked to stay at home, an increase of the use of heating systems during this period has been observed. Some first estimates in France showed that an increase of 20% of emissions could be observed. Then, for each country a factor $-f_7/4$ is applied for the residential sector (SNAP 2), so that the more traffic emissions are reduced the more residential emission increase. This formula caps the residential increase to $+25\%$.

This method provides daily multiplication factors for each country and activity sectors. Application of these factors to the ‘business as usual’ emissions that are used for the REF emission dataset allows to produce emissions for the CVD simulation that include the effect of lockdown measures.

2.3. Observations

This study focuses on air quality, then on the surface concentrations of pollutants. For the comparison of the modelling results to observations, we thus prefer comparisons to in-situ measurements and as measured for air quality calculations to have real concentrations values. The European Environment Agency (EEA, <https://www.eea.europa.eu>) provides a full set of hourly data for several pollutants such as particulate matter $\text{PM}_{2.5}$ and PM_{10} , ozone (O_3) and nitrogen dioxide (NO_2) for a large number of stations in Western Europe. For the results presented in this study, we used only the background urban, rural and suburban stations, considering that the industrial and traffic has a spatial representativity too different to be compared to the model with its spatial resolution of $\Delta x = 20$ km. The number of available stations is different for each pollutants and for the period of March 2020 we used the data from 1456 stations for NO_2 , 1443 for O_3 , 799 for PM_{10} and 399 for $\text{PM}_{2.5}$.

3. Results

Results are presented as comparisons of simulations to surface measurements. The two simulations are REF (reference case) and CVD (with the lockdown scenario on emissions) and the pollutants are $PM_{2.5}$, PM_{10} , O_3 and NO_2 . Results are presented under three different formats: daily average time-series compared to measurement stations, daily average percentage of changes in concentrations aggregated per countries and maps of differences.

3.1. Impact for selected sites

The following Figures show time-series of surface concentrations for three pollutants, NO_2 , O_3 and PM_{10} . The stations were chosen because they were spread all over Western Europe, they are characteristic of 'background and rural' environment (in line with a 20 km model resolution) and have, as much as possible, data for all three pollutants. The list of stations is presented in Table 1. This table lists the stations with their name, country, longitude ($^\circ$), latitude ($^\circ$) and altitude above sea level (m ASL).

For NO_2 , Fig. 3, it can be seen that all stations show surface concentrations values with higher measured concentrations than modelled. For this chemical species, this bias is normal and is due to the 20 km resolution of the model. Even if the stations are of background and rural type, NO_2 remains a pollutant whose representativeness is spatially limited. Close to emission sources, this pollutant is mainly primary and represents well the emission reductions related to lockdown. The differences between REF and CVD simulation show the start dates of the emission reductions as they have been put in the scenario. In Italy and the Netherlands, differences in concentrations can be seen from the beginning of March. In France, Spain and Portugal, the impact is visible in mid March. For all stations, the impact varies from day to day and does not become constant at the end of the month. The most important differences can reach $10 \mu g m^{-3}$ as a daily average.

For ozone, Fig. 4, a secondary pollutant with a longer lifetime than NO_2 and greater long-range transport capacity, the impact is lower in concentrations. Time series are presented for the same stations as NO_2 to ease the comparisons. The model bias is lower in comparison with observations. The REF and CVD simulations also show fewer differences, with maximum values of the order of 5 to $10 \mu g m^{-3}$. For several sites, such as Vercelli, Chamforgeuil and Fernando, higher ozone values are measured and modelled at the end of the month, between 20 and 25 March. At these sites, no particular increase or decrease in ozone concentrations due to the lockdown is noted.

On Fig. 5, the differences between the REF and CVD simulations for PM_{10} are, as for ozone, quite small. Comparisons between measurements and simulations are good and no particular bias is noted. As for ozone, there is a peak concentration between 24 and 29 March. This seems to correspond to a particulate episode over a large part of Europe since the stations of Spreewald, Kosetice, Illmitz, Vredepeel are

impacted. But the Fernando station in Portugal does not show this increase. For this station, we see on the contrary a significant peak of PM_{10} on 18 March which is measured and well modelled, with concentrations of $60 \mu g m^{-3}$. However, for this peak, there is no difference in the scenarios, so it is probably a peak of natural origin. For all stations, the difference between the scenarios remains small and is of the order of a few $\mu g m^{-3}$.

3.2. Impact per countries

The time series in Fig. 6 represent the daily average percentages of reduction in pollutant concentrations (NO_2 , ozone and $PM_{2.5}$) for different European countries defined by the concentration ratio. Concentrations are represented separately for urban and rural areas in each country, using the landuse fractions (Fig. 1).

For NO_2 , a local pollutant, Germany and the Netherlands reach concentration reductions of -15 to -30% , while the other countries show concentration reductions in the range of -35 to -45% on average. This is in line with less strict or different lockdown measures in the northern countries somehow less strict. In all cases, the impacts are clearly visible in relation to the different starting dates lockdown by country, with Italy adopting measures as early as 1 March, France as early as 14 March, etc.

For ozone, a pollutant that is more regional than local, the impact of lockdown on concentrations is much smaller, with a very slight decrease observed in rural areas, whereas concentrations can significantly increase in urban areas due to the effect of chemical titration, which is cancelled out by the strong reductions in nitrogen oxide emissions. Ozone is in fact a so-called secondary air pollutant which is part of a chemical cycle of formation and destruction involving nitrogen oxides and volatile organic compounds.

For $PM_{2.5}$, reductions in concentrations are weak, between -5 and -10% . Emissions of primary particles from residential heating, which was still in use and certainly increasing in the second half of March, were able to partly offset the reductions of the formation of secondary particles usually resulting from the start of agricultural activity (fertilizer spreading) at the end of winter. Emissions from the agricultural sector were not reduced in these simulations. Ammonia emitted by the agricultural sector and nitrogen oxides emitted by the remaining sources (agriculture, industry, maritime traffic, other remaining traffic emissions, etc.) contribute to the formation of secondary fine particulate matter.

Another way to express the results is presented in Table 2. In this case, the daily delta of concentrations (CVD-REF) is calculated for each country: over the whole month of March 2020, the maximum, in absolute values, is presented. Results are presented for NO_2 , $PM_{2.5}$ and O_3 .

Ozone is one of the most complicated chemical species in the atmosphere. It is a regionally sensitive secondary pollutant, so it is better mixed in the atmosphere compared to other locally sensitive species such as NO_x . Its concentration can depend on several factors simultaneously: NO_x availability, rural/urban configuration of the area, VOC availability and meteorological conditions ((Sillman et al., 2003), (Seinfeld and Pandis, 2006)). The ratio of VOC/ NO_x concentration decides the chemical regime affecting ozone production: High NO_x emissions mean a VOC-limited chemical regime, while large VOC emissions (depending on HO_x availability as well) mean the contrary ((Kwok et al., 2015)). This means, simply put and in most cases, in urban areas where NO_x emissions are dominant in normal meteorological conditions a VOC-limited regime is seen, while in rural areas a NO_x -limited regime is observed. Therefore, when encountering a situation where NO_x emissions are decreasing significantly (like in CVD simulations in our study) an increase in ozone concentrations is expected in urban areas when we're in a VOC-limited chemical regime and a decrease is expected in rural areas in a NO_x -limited regime. Table 2 shows the maximum changes for ozone on the national level differentiated for each country on the rural and urban, where the aforementioned behavior is partially seen, the inconsistencies can be explained by the fact that

Table 1

Names and locations of the EEA (European Environment Agency) stations used for model comparisons to surface concentrations. The stations are listed in alphabetical order. Longitude ($^\circ$), latitude ($^\circ$) and altitude above sea level (m ASL) is indicated for each station.

Site	Country	Longitude ($^\circ$)	Latitude ($^\circ$)	Altitude (m ASL)
Champforgeuil	France	4.83	46.82	185
ElsTorms	Spain	0.73	41.39	470
Enzenkirchen	Austria	13.67	48.39	525
Fernando	Portugal	-8.69	38.63	57
Illmitz	Austria	16.76	47.77	117
Kosetice	Czech Rep.	15.08	49.57	535
Spreewald	Germany	14.05	51.89	52
Vercelli	Italy	8.40	45.31	131
Vredepeel	Netherlands	5.85	51.54	28

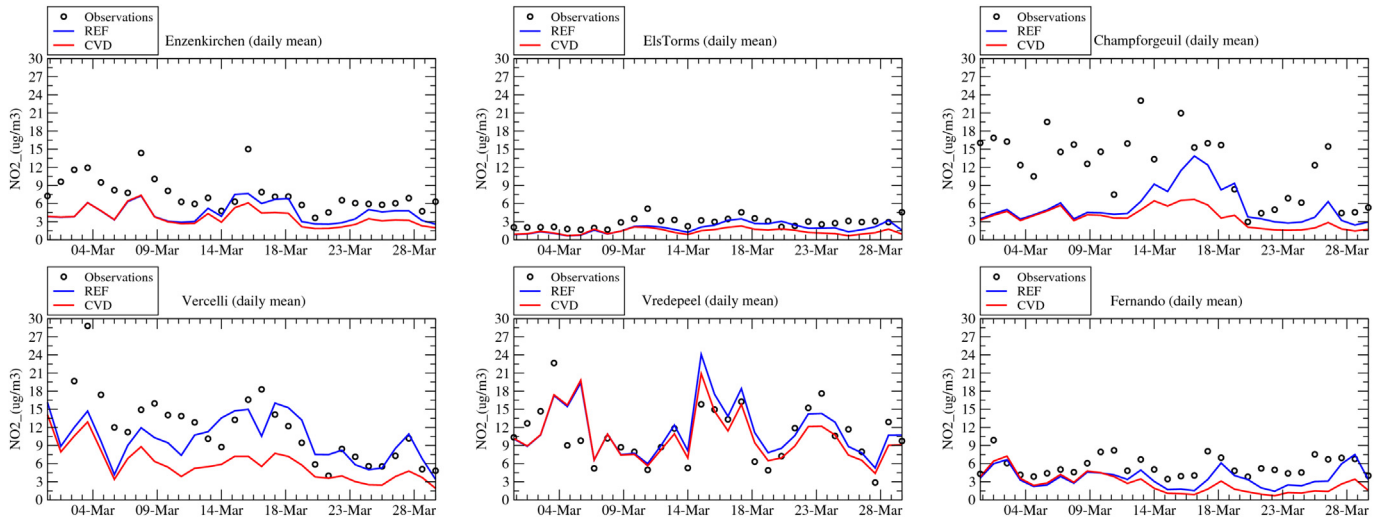


Fig. 3. Time-series of daily average surface concentrations of NO₂ (µg m⁻³). Stations are representative of several locations in Western Europe and are all classified by EEA as 'background' and 'rural'.

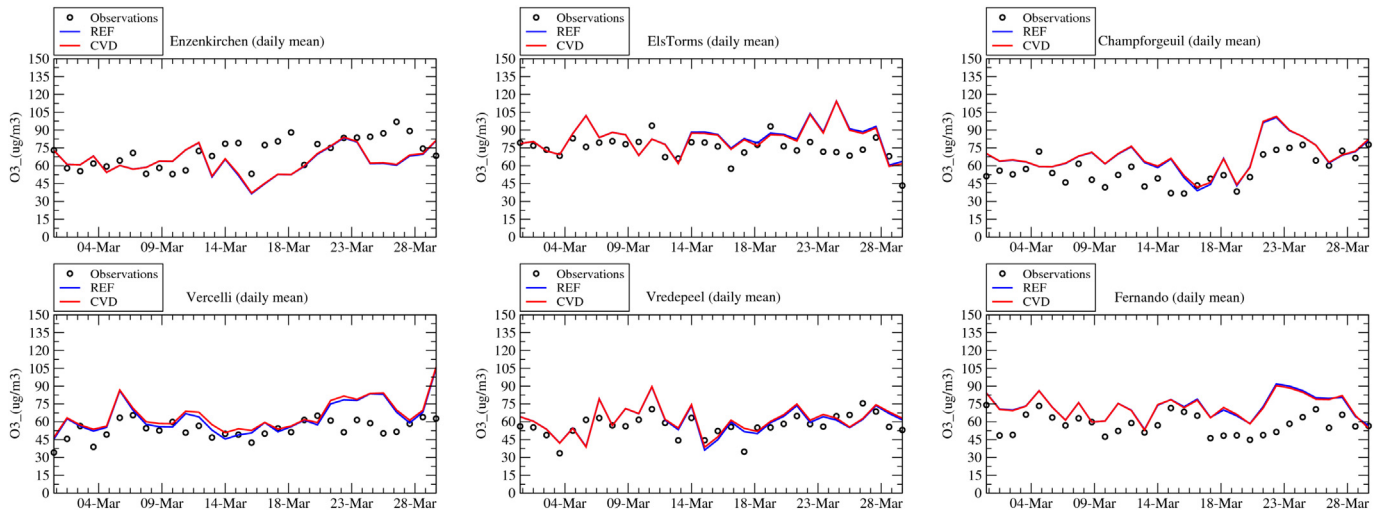


Fig. 4. Time-series of daily average surface concentrations of O₃ (µg m⁻³). Stations are representative of several locations in Western Europe and are all classified by EEA as 'background' and 'rural'.

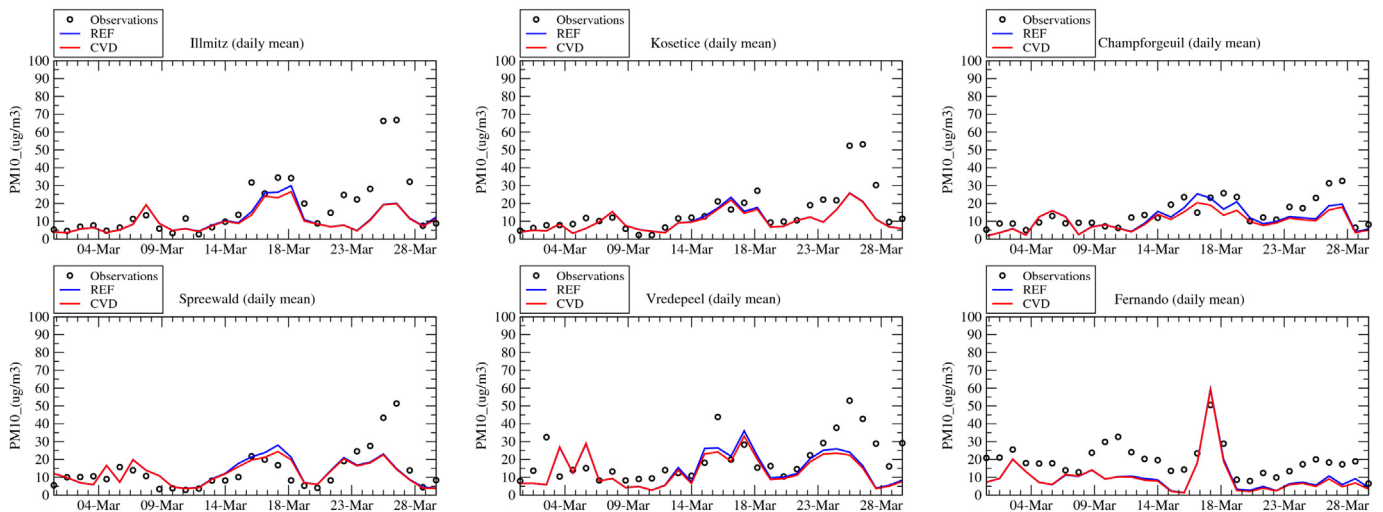


Fig. 5. Time-series of daily average surface concentrations of PM₁₀. Stations are representative of several locations in Western Europe and are all classified by EEA as 'background' and 'rural'.

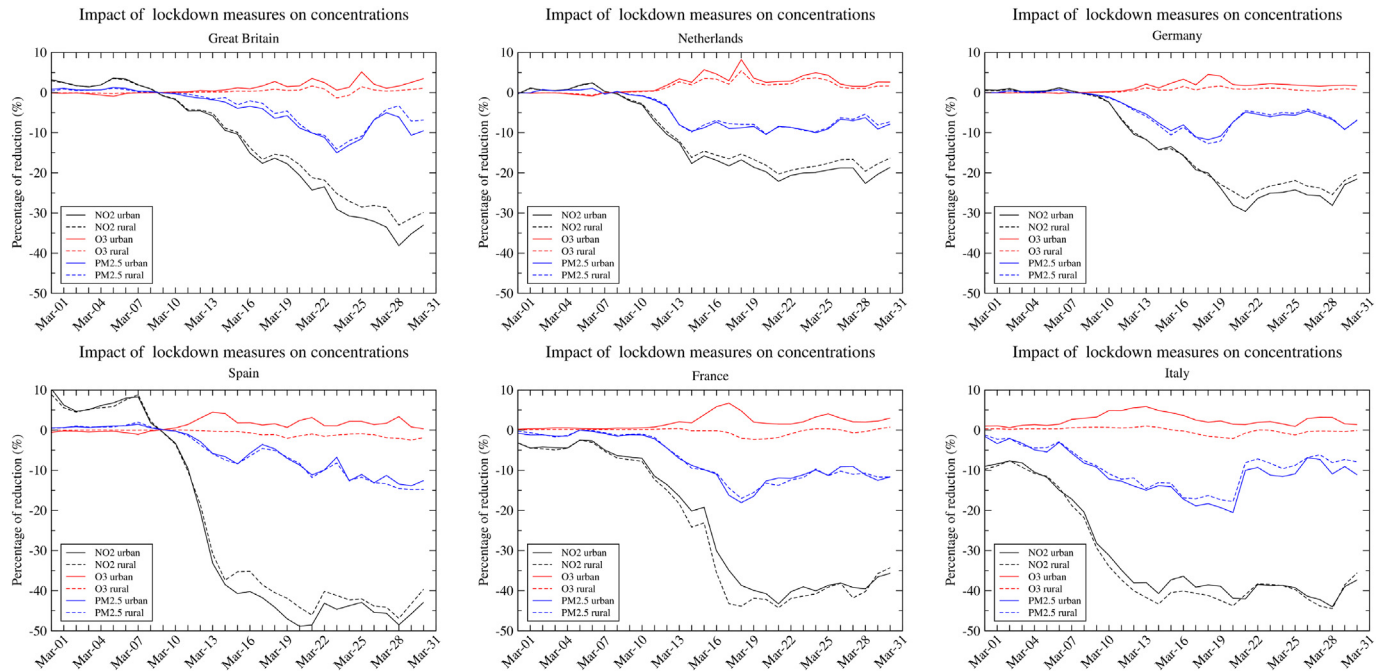


Fig. 6. Time-series of daily percentage of reduction (CVD-REF) calculated for each country (urban and rural areas) and three pollutants: PM_{2.5}, NO₂ and O₃. Results are presented for the whole month of March 2020 and for Great Britain, Netherlands, Germany, Spain, France and Italy.

ozone is usually regionally well-mixed therefore it does not show local signals that often (especially in lower horizontal resolutions). The concentration of ozone in different chemical regimes has been explored in detail in models in many publications (e.g. (Beekmann and Vautard, 2010) and (Wilson et al., 2012) in case of the CHIMERE model).

For NO₂, the daily delta is negative for all countries, ranging from −13.0% (urban) and −9.7% (rural) for the lowest delta in Sweden to

−57.8% (urban) and −53.6% in Portugal. For PM_{2.5}, the daily delta is lower and may be negative or positive depending on the country. The largest negative change is −23.5% (urban) and −13.0% (rural) in Portugal when the largest positive change is +4.0 (urban) but −4.6% in Poland. This positive change is the only one in Europe. For ozone, the daily delta oscillates between negative and positive values, but changes are not important. The variability is from −2.7% (urban) and −2.34% (rural) in Ireland to +17.6% (urban) and +6.6% (rural) in Belgium. It is noteworthy that the neighbouring country, The Netherlands, also has one of the highest increase in urban areas for ozone. For all countries and for ozone, the daily delta maxima are often between ±0 to 5%. Changes are the most important for NO₂ with percentages between −10% to −40% in urban areas, where the major part of emissions are reduced in the CVD emissions inventory.

Table 2

Maximum daily delta (CVD-REF) of concentrations (%) reached in March 2020 for the main European countries within the domain. A negative value is for a reduction of concentration, a positive value is for an increase of concentration. Note that “BosniaHzgv” stands for “Bosnia and Herzegovina”, “UnitedKgd” for “United Kingdom”.

Country	NO ₂		PM _{2.5}		O ₃	
	Urban	Rural	Urban	Rural	Urban	Rural
Austria	−37.1	−37.8	−10.3	−11.2	+6.4	+0.64
Belgium	−34.8	−33.6	−13.4	−15.7	+17.6	+6.60
Bosnia Hzgv	−43.2	−16.2	−5.8	−4.1	−1.5	−2.17
Bulgaria	−38.5	−33.4	−5.3	−4.8	−2.1	−2.45
Croatia	−37.5	−23.1	−11.6	−6.6	−1.5	−1.65
Czech Rep.	−18.1	−21.6	−5.7	−8.5	+1.2	+0.63
Denmark	−19.8	−13.6	−6.3	−6.7	+1.5	+0.27
France	−43.2	−43.8	−18.0	−17.0	+6.7	+0.72
Germany	−29.5	−25.4	−11.7	−12.7	+4.5	+0.73
Greece	−44.6	−27.2	−11.0	−4.6	+5.2	−2.37
Hungary	−22.6	−24.8	−4.7	−7.1	−0.7	−1.60
Italy	−44.0	−44.4	−20.5	−17.8	+5.8	−0.08
Ireland	−37.3	−29.5	−11.1	−11.7	−2.7	−2.34
Lithuania	−26.5	−24.5	−4.9	−4.9	+0.8	+0.04
Netherlands	−22.6	−16.3	−10.4	−10.3	+8.2	+5.41
Norway	−24.0	−20.4	−6.7	−6.5	+1.3	+0.07
Poland	−27.0	−25.6	+4.0	−4.6	+3.7	+0.65
Portugal	−57.8	−53.6	−23.5	−13.0	+8.1	−2.39
Romania	−28.6	−29.4	−4.8	−4.8	−1.6	−1.82
Russia	−25.4	−17.6	−10.0	−2.5	+1.6	+0.04
Serbia	−26.7	−19.3	−5.9	−2.4	−1.7	−2.37
Slovakia	−23.8	−23.8	−8.3	−7.6	−0.9	−1.38
Slovenia	−40.7	−29.1	−18.4	−16.3	+2.1	−1.52
Spain	−48.8	−46.8	−13.8	−14.5	+4.4	−2.04
Sweden	−13.0	−9.7	−5.4	−5.5	+0.7	+0.01
Switzerland	−31.4	−33.0	−18.0	−22.0	+1.8	+0.50
United Kgd	−38.1	−29.8	−15.0	−14.0	+5.1	+1.06

3.3. The specific episode of 28 March 2020

From 23 to 28 March 2020, a pollution episode with large concentrations of particular matter has been observed in several countries including France (Fig. 5). For France, reports from operational forecasters have indicated that this pollution peak was essentially due to two factors: strong emissions from residential heating, with an important contribution of wood burning, and inputs of fertilizers on the crops. Fig. 7 shows the effect of lockdown measures on the main pollutants for 28 March 2020. As expected due to the massive reduction in traffic emissions, nitrogen dioxide concentrations were largely impacted by containment measures with average decreases of 5 to 10 $\mu\text{g m}^{-3}$ in urban areas. Ozone is positively affected by lockdown measures urban areas but negatively in rural areas, as we have also observed at national level (Fig. 6). Regarding particular matter, which were the cause of poor air quality during these days, the decrease due to lockdown is only modest, and explained essentially by a negative impact of lockdown on nitrate concentrations. No particular impact of lockdown on agricultural activities has been reported and fertilizer input onto the cultivated fields has been performed as usual by the farmers. As nitrates being a product of NO₂ oxidation, this reduced contribution of nitrate to the PM peak in the days preceding can be explained as a consequence of reduce emissions of nitrogen dioxide from traffic. This brief episode was also marked by

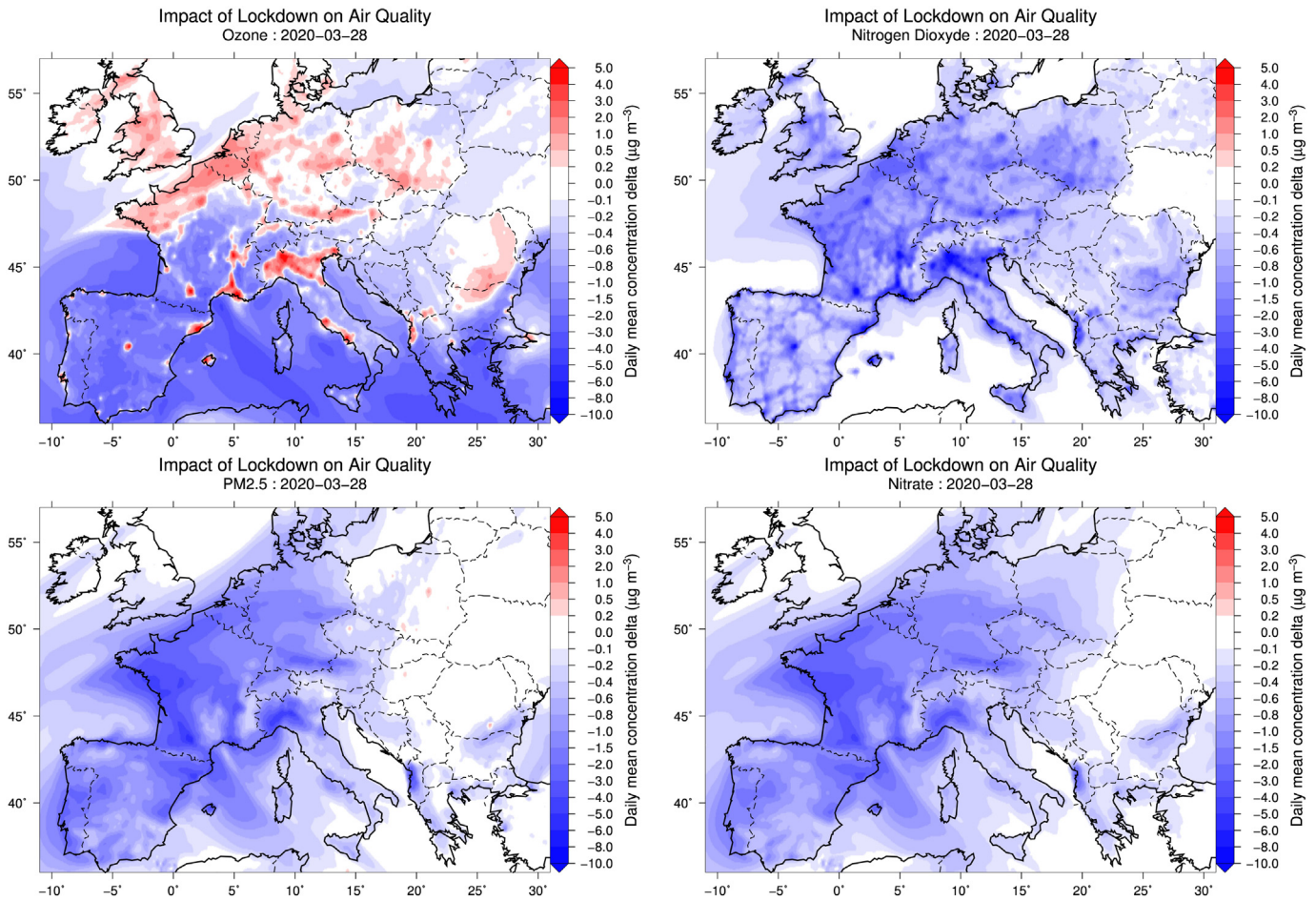


Fig. 7. Maps of differences (CVD-REF) of daily average surface concentrations ($\mu\text{g m}^{-3}$) for the 28 March 2020 and for ozone, nitrogen oxide, $\text{PM}_{2.5}$ and PM_{10} .

the appearance of larger terrigenous mineral particles captured by the model (not shown here), the origin of which is still to be clarified. However, a possible outbreak of mineral dust from Ukraine or the south of Russia or even Kazakhstan could be the reason as it has already observed in 2007 in such strong easterly air mass fluxes (Bessagnet et al., 2008).

3.4. Statistical scores over Europe

In order to summarize all results, statistical scores are calculated using all stations over the modelled domain. Results are presented in Table 3.

The NO_2 scores show that the closer to reality scenario simulation, CVD, does not improve the RMSE and the bias: the bias goes from -14.43 to $-17.63 \mu\text{g m}^{-3}$ for 'all' stations. On the other hand, there is an improvement of time correlation, from 0.36 to 0.43 for 'all'. This is due to the reduction of emissions for some activity sectors only and therefore a change in the monthly profile of emissions. We therefore have a correlation closer to reality. The biggest improvement is logically in urban areas, from 0.37 to 0.44, where these emissions are the most important and where the scenario has the largest effect.

For ozone, the bias is reduced for all areas: rural, suburban and urban. But the correlation is less good (from 0.29 to 0.26 for all stations). The RMSE is higher but the difference is not significant: from 15.52 to $15.59 \mu\text{g m}^{-3}$ for 'all'. However, the bias decreases, from 2.59 to $2.21 \mu\text{g m}^{-3}$ for all stations and, more particularly, from 0.31 to $-0.07 \mu\text{g m}^{-3}$ in rural areas.

For PM, the behavior of the model is similar for $\text{PM}_{2.5}$ and PM_{10} . The correlation is good for both simulations and the different environments.

Table 3

Statistical scores calculated by comparison between surface observations for several stations in Europe and the corresponding model daily mean value, for the simulations REF and CVD. RMSE and bias are in $\mu\text{g m}^{-3}$ and Pearson's temporal correlation between -1 and 1. Statistical scores are presented for NO_2 , O_3 , $\text{PM}_{2.5}$ and PM_{10} .

	REF			CVD		
	RMSE	Bias	R_t	RMSE	Bias	R_t
NO_2						
All	20.77	-14.43	0.37	22.35	-17.63	0.43
Rural	8.16	-3.68	0.35	8.74	-5.10	0.37
Suburban	20.86	-14.06	0.37	22.10	-17.20	0.44
Urban	25.96	-20.53	0.38	27.92	-23.42	0.46
O_3						
All	15.53	2.59	0.29	15.59	2.21	0.26
Rural	14.96	0.31	0.25	15.16	-0.07	0.23
Suburban	15.52	2.65	0.28	15.67	2.31	0.25
Urban	15.89	4.01	0.31	16.07	3.66	0.28
$\text{PM}_{2.5}$						
All	6.31	-0.24	0.70	6.34	-0.77	0.70
Rural	5.97	1.27	0.70	5.74	0.80	0.70
Suburban	7.66	0.65	0.68	7.18	0.02	0.66
Urban	6.21	-1.36	0.70	6.41	-2.08	0.71
PM_{10}						
All	9.50	-5.47	0.69	9.89	-6.07	0.69
Rural	8.37	-3.46	0.67	8.39	-4.20	0.67
Suburban	10.08	-5.19	0.67	10.48	-5.88	0.68
Urban	9.68	-6.28	0.71	10.27	-7.02	0.71

There is no significant change between REF and CVD. For PM_{2.5}, we note a degradation of the bias for all stations, from $-0.24 \mu\text{g m}^{-3}$ to $-0.77 \mu\text{g m}^{-3}$, and this is particularly true in urbanized environment with an increase of the bias from -1.36 to $-2.08 \mu\text{g m}^{-3}$.

4. Conclusions

This first modelling work in Europe provides a rigorous framework for studying the effects of containment on air quality by avoiding meteorological biases (comparison here over identical periods) and biases intrinsic to the model (when focussing on the analysis of differences). Our results given at a resolution of 20 km show decreases in NO₂ concentrations ranging from -30% to -50% in all western Europe countries. Ozone concentrations have been differently affected in urban areas throughout Western Europe by lockdown measures with increase of concentrations. The effect on fine particle concentrations has been less pronounced than on NO₂ (-5 to -15%). This can be explained by the fact that traffic is not the sole source of fine particles. Particularly during this season, residential heating emissions, which are a very substantial contributor to PM concentrations in western Europe is supposed to increase by lockdown measures since European citizens have been instructed to stay at home as much as possible. Also, agricultural emissions due to fertilizer spreading is known to be a strong source of ammonium nitrate in western European countries in late winter and early springtime, they have not been affected by lockdown measures. These preliminary results are encouraging and in agreement with studies based on comparisons with satellite and station measurements. Further analyses will have to be carried out to better understand the weight of sectors in these modelled differences. A refinement of assumptions on emissions adjustment due to the lockdown measures will be necessary to improve results robustness.

CRedit authorship contribution statement

Laurent Menut: Conceptualization, Methodology, Writing - original draft, Formal analysis. **Bertrand Bessagnet:** Conceptualization, Methodology, Writing - original draft, Formal analysis. **Guillaume Siour:** Conceptualization, Methodology, Writing - original draft, Formal analysis. **Sylvain Mailler:** Conceptualization, Methodology, Writing - original draft, Formal analysis. **Romain Pennel:** Conceptualization, Methodology, Writing - original draft, Formal analysis. **Arineh Cholakian:** Conceptualization, Methodology, Writing - original draft, Formal analysis.

Declaration of competing interest

The authors declare that they have no known competing financial interests or personal relationships that could have appeared to influence the work reported in this paper.

Acknowledgements

This work was performed using resources from GENCI-TGCC (Grant A0070110274). Meteorological simulations were performed by forcing WRF with NCEP model fields, (NCAR/UCAR, 2000). The authors are grateful to the EEA (European Environmental Agency) for maintaining and providing the surface concentrations of criteria pollutants over Europe.

References

Alfaro, S.C., Gomes, L., 2001. Modeling mineral aerosol production by wind erosion: emission intensities and aerosol size distribution in source areas. *J. Geophys. Res.* 106 (18) (075–18, 084).

Bauwens, M., Compennolle, S., Stavrakou, T., Muller, J.F., van Gent, J., Eskes, H., Levelt, P.F., Van Der, A.R., Veeffkind, J.P., Vlietinck, J., Yu, H., Zehner, C., 2020. Impact of coronavirus

outbreak on no2 pollution assessed using tropomi and omi observations. *Geophys. Res. Lett.* 47, e2020GL087978. <https://doi.org/10.1029/2020GL087978>.

Beekmann, M., Vautard, R., 2010. A modelling study of photochemical regimes over Europe: robustness and variability. *Atmos. Chem. Phys.* 10, 10067–10084. <https://doi.org/10.5194/acp-10-10067-2010>.

Bessagnet, B., Menut, L., Aymoz, G., Chepfer, H., Vautard, R., 2008. Modelling dust emissions and transport within Europe: the Ukraine March 2007 event. *J. Geophys. Res.* 113, D15202. <https://doi.org/10.1029/2007JD009541>.

Bessagnet, B., Seigneur, C., Menut, L., 2010. Impact of dry deposition of semi-volatile organic compounds on secondary organic aerosols. *Atmos. Environ.* 44, 1781–1787. <https://doi.org/10.1016/j.atmosenv.2010.01.027>.

Bessagnet, B., Pirovano, G., Mircea, M., Cuvelier, C., Aulinger, A., Calori, G., Ciarelli, G., Manders, A., Stern, R., Tsyro, S., Garcia Vivanco, M., Thunis, P., Pay, M.T., Colette, A., Couvidat, F., Meleux, F., Rouil, L., Ung, A., Aksoyoglu, S., Baldasano, J.M., Bieser, J., Briganti, G., Cappelletti, A., D'Isidoro, M., Finardi, S., Kranenburg, R., Silibello, C., Carnevale, C., Aas, W., Dupont, J.C., Fagerli, H., Gonzalez, L., Menut, L., Prévôt, A., Roberts, P., White, L., 2016. Presentation of the EURODELTA III intercomparison exercise - evaluation of the chemistry transport models' performance on criteria pollutants and joint analysis with meteorology. *Atmos. Chem. Phys.* 16, 12667–12701. <https://doi.org/10.5194/acp-16-12667-2016>.

Bessagnet, B., Menut, L., Lapere, R., Couvidat, F., Jaffrezo, J.L., Mailler, S., Favez, O., Pennel, R., Siour, G., 2020. High resolution chemistry transport modeling with the on-line CHIMERE-WRF model over the French Alps-analysis of a feedback of surface particulate matter concentrations on mountainous meteorology. *Atmosphere* 11. <https://doi.org/10.3390/atmos11060565>.

Cholakian, A., Beekmann, M., Colette, A., Coll, I., Siour, G., Sciare, J., Marchand, N., Couvidat, F., Pey, J., Gros, V., Sauvage, S., Michoud, V., Sellegri, K., Colomb, A., Sartelet, K., Langley DeWitt, H., Elser, M., Prévôt, A.S.H., Szidat, S., Dulac, F., 2018. Simulation of fine organic aerosols in the western Mediterranean area during the ChArMEX 2013 summer campaign. *Atmos. Chem. Phys.* 18, 7287–7312.

Collivignarelli, M.C., Abba, A., Bertanza, G., Pedrazzani, R., Ricciardi, P., Miino, M.C., 2020. Lockdown for CoViD-2019 in Milan: what are the effects on air quality? *Sci. Total Environ.*, 139280 <https://doi.org/10.1016/j.scitotenv.2020.139280>.

Couvidat, F., Bessagnet, B., Garcia-Vivanco, M., Real, E., Menut, L., Colette, A., 2018. Development of an inorganic and organic aerosol model (CHIMERE 2017β v1.0): seasonal and spatial evaluation over Europe. *Geosci. Model Dev.* 11, 165–194. <https://doi.org/10.5194/gmd-11-165-2018>.

Granier, C., Darras, S., van der Gon, H.D., Doubalova, J., Elguindi, N., Galle, B., Gauss, M., Guevara, M., Jalakanen, J.P., Kuenen, J., Liousse, C., Quack, B., Simpson, D., Sindelarova, K., 2019. The Copernicus atmosphere monitoring service global and regional emissions (April 2019 version). Copernicus <https://doi.org/10.24380/d0bn-kx16>.

Guenther, A., Karl, T., Harley, P., Wiedinmyer, C., Palmer, P., Geron, C., 2006. Estimates of global terrestrial isoprene emissions using MEGAN (model of emissions of gases and aerosols from nature). *Atmos. Chem. Phys.* 6, 3181–3210.

Honoré, C., Rouil, L., Vautard, R., Beekmann, M., Bessagnet, B., Dufour, A., Elichegaray, C., Flaud, J., Malherbe, L., Meleux, F., Menut, L., Martin, D., Peuch, A., Peuch, V., Poisson, N., 2008. Predictability of European air quality: the assessment of three years of operational forecasts and analyses by the PREV'AIR system. *J. Geophys. Res.* 113, D04301. <https://doi.org/10.1029/2007JD008761>.

Kalnay, E., Kanamitsu, M., Kistler, R., Collins, W., Deaven, D., Gandin, L., Iredell, M., Saha, S., White, G., Woollen, J., Zhu, Y., Chelliah, M., Ebisuzaki, W., Higgins, W., Janowiak, J., Mo, K., Ropelewski, C., Wang, J., Leetmaa, A., Reynolds, R., Jenne, R., Joseph, D., 1996. The NCEP/NCAR 40-year reanalysis project. *Bull. Am. Meteorol. Soc.*, 437–471 [https://doi.org/10.1175/1520-0477\(1996\)077](https://doi.org/10.1175/1520-0477(1996)077).

Kwok, R.H.F., Baker, K.R., Napelenok, S.L., Tonnesen, G.S., 2015. Photochemical grid model implementation and application of VOC, NO_x, and O₃ source apportionment. *Geosci. Model Dev.* 8, 99–114. <https://doi.org/10.5194/gmd-8-99-2015>.

Mailler, S., Menut, L., di Sarra, A.G., Becagli, S., Di Iorio, T., Bessagnet, B., Briant, R., Formenti, P., Doussin, J.F., Gómez-Amo, J.L., Mallet, M., Rea, G., Siour, G., Sferlazzo, D.M., Traversi, R., Udisti, R., Turquety, S., 2016. On the radiative impact of aerosols on photolysis rates: comparison of simulations and observations in the lampedusa island during the charmex/adrimed campaign. *Atmos. Chem. Phys.* 16, 1219–1244. <https://doi.org/10.5194/acp-16-1219-2016>.

Mailler, S., Menut, L., Khvorostyanov, D., Valari, M., Couvidat, F., Siour, G., Turquety, S., Briant, R., Tuccella, P., Bessagnet, B., Colette, A., Léinois, L., Markakis, K., Meleux, F., 2017. CHIMERE-2017: from urban to hemispheric chemistry-transport modeling. *Geosci. Model Dev.* 10, 2397–2423. <https://doi.org/10.5194/gmd-10-2397-2017>.

Marécal, V., Peuch, V.H., Andersson, C., Andersson, S., Arteta, J., Beekmann, M., Benedictow, A., Bergström, R., Bessagnet, B., Cansado, A., Chéroux, F., Colette, A., Coman, A., Curier, R.L., Denier van der Gon, H.A.C., Drouin, A., Elbern, H., Emili, E., Engelen, R.J., Eskes, H.J., Foret, G., Friese, E., Gauss, M., Giannaros, C., Guth, J., Joly, M., Jaumouillé, E., Josse, B., Kadygrov, N., Kaiser, J.W., Krajsek, K., Kuenen, J., Kumar, U., Liora, N., Lopez, E., Malherbe, L., Martinez, I., Melas, D., Meleux, F., Menut, L., Moinat, P., Morales, T., Parmentier, J., Piacentini, A., Plu, M., Poupkou, A., Queguiner, S., Robertson, L., Rouil, L., Schaap, M., Segers, A., Sofiev, M., Tarasson, L., Thomas, M., Timmermans, R., Valdebenito, A., van Velthoven, P., van Versendaal, R., Vira, J., Ung, A., 2015. A regional air quality forecasting system over Europe: the MACC-II daily ensemble production. *Geosci. Model Dev.* 8, 2777–2813. doi:<https://doi.org/10.5194/gmd-8-2777-2015>.

Mareckova, K., Pinterits, M., Ullrich, B., Wankmueller, R., Gaisbauer, S., 2019. EMEP Inventory Review 2019 Review of Emission Data Reported under the LRTAP Convention and NEC Directive. European Environment Agency and CEIP, p. 54.

Menut, L., Bessagnet, B., 2010. Atmospheric composition forecasting in Europe. *Ann. Geophys.* 28, 61–74.

- Menut, L., Vautard, R., Flamant, C., Abonne, C., Beekmann, M., Chazette, P., Flamant, P., Gombert, D., Guédalia, D., Lefebvre, M., Lossec, D., M., B., Mégie, G., Perros, P., Sicard, M., Toupance, G., 2000. Measurements and modelling of atmospheric pollution over the Paris area: an overview of the ESQUIF project. *Ann. Geophys.* 18, 1467–1481.
- Menut, L., Coll, I., Cautenet, S., 2005a. Impact of meteorological data resolution on the forecasted ozone concentrations during the ESCOMPTE IOP 2a and 2b. *Atmos. Res.* 74, 139–159.
- Menut, L., Schmechtig, C., Marticorena, B., 2005b. Sensitivity of the sandblasting fluxes calculations to the soil size distribution accuracy. *J. Atmos. Ocean. Technol.* 22, 1875–1884.
- Menut, L., Goussebaile, A., Bessagnet, B., Khvorostyanov, D., Ung, A., 2012. Impact of realistic hourly emissions profiles on modelled air pollutants concentrations. *Atmos. Environ.* 49, 233–244. <https://doi.org/10.1016/j.atmosenv.2011.11.057>.
- Menut, L., Bessagnet, B., Khvorostyanov, D., Beekmann, M., Blond, N., Colette, A., Coll, I., Curci, G., Foret, F., Hodzic, A., Mailler, S., Meleux, F., Monge, J., Pison, I., Siour, G., Turquety, S., Valari, M., Vautard, R., Vivanco, M., 2013. CHIMERE 2013: a model for regional atmospheric composition modelling. *Geosci. Model Dev.* 6, 981–1028. <https://doi.org/10.5194/gmd-6-981-2013>.
- Menut, L., Mailler, S., Siour, G., Bessagnet, B., Turquety, S., Rea, G., Briant, R., Mallet, M., Sciare, J., Formenti, P., Meleux, F., 2015a. Ozone and aerosol tropospheric concentrations variability analyzed using the ADRIMED measurements and the WRF and CHIMERE models. *Atmos. Chem. Phys.* 15, 6159–6182. <https://doi.org/10.5194/acp-15-6159-2015>.
- Menut, L., Rea, G., Mailler, S., Khvorostyanov, D., Turquety, S., 2015b. Aerosol forecast over the Mediterranean area during July 2013 (ADRIMED/CHARMEX). *Atmos. Chem. Phys.* 15, 7897–7911. <https://doi.org/10.5194/acp-15-7897-2015>.
- Menut, L., Tuccella, P., Flamant, C., Deroubaix, A., Gaetani, M., 2019. The role of aerosol-radiation-cloud interactions in linking anthropogenic pollution over southern West Africa and dust emission over the Sahara. *Atmos. Chem. Phys.* 19, 14657–14676. <https://doi.org/10.5194/acp-19-14657-2019>.
- Monahan, E.C., 1986. In the Role of Air-Sea Exchange in Geochemical Cycling. Kluwer Academic Publishers, Dordrecht, Holland, pp. 129–163 chapter The ocean as a source of atmospheric particles.
- Muhammad, S., Long, X., Salman, M., 2020. COVID-19 pandemic and environmental pollution: a blessing in disguise? *Sci. Total Environ.* 728, 138820. <https://doi.org/10.1016/j.scitotenv.2020.138820>.
- NCAR/UCAR, 2000. NCEP FNL Operational Model Global Tropospheric Analyses, Continuing from July 1999, Research Data Archive at the National Center for Atmospheric Research. Computational and Information Systems Laboratory <https://doi.org/10.5065/D6M043C6>.
- Petetin, H., Bowdalo, D., Soret, A., Guevara, M., Jorba, O., Serradell, K., Pérez García-Pando, C., 2020. Meteorology-normalized impact of COVID-19 lockdown upon NO₂ pollution in Spain. *Atmospheric Chemistry and Physics Discussions* 2020, 1–29. <https://doi.org/10.5194/acp-2020-446>.
- Pirovano, G., Coll, I., Bedogni, M., Alessandrini, S., Costa, M., Gabusi, V., Lasry, F., Menut, L., Vautard, R., 2007. On the influence of meteorological input on photochemical modelling of a severe episode over a coastal area. *Atmos. Environ.* 41, 6445–6464.
- Rouil, L., Honoré, C., Vautard, R., Beekmann, M., Bessagnet, B., Malherbe, L., Meleux, F., Dufour, A., Ellichgaray, C., Flaud, J., Menut, L., Martin, D., Peuch, A., Peuch, V., Poisson, N., 2009. PREV'AIR: an operational forecasting and mapping system for air quality in Europe. *BAMS* 90, 73–83. <https://doi.org/10.1175/2008BAMS2390.1>.
- Seinfeld, J., Pandis, S., 2006. *Atmospheric Chemistry and Physics: From Air Pollution to Climate Change*. 2nd edition. Wiley-Interscience, Hoboken.
- Sharma, S., Zhang, M., Anshika, Gao, J., Zhang, H., Kota, S.H., 2020. Effect of restricted emissions during COVID-19 on air quality in India. *Sci. Total Environ.* 728, 138878. <https://doi.org/10.1016/j.scitotenv.2020.138878>.
- Shi, X., Brasseur, G.P., 2020. The response in air quality to the reduction of chinese economic activities during the covid-19 outbreak. *Geophys. Res. Lett.* 47, e2020GL088070. <https://doi.org/10.1029/2020GL088070>.
- Sillman, S., Vautard, R., Menut, L., Kley, D., 2003. O₃-NO_x-VOC sensitivity indicators in Paris: results from models and ESQUIF measurements. *J. Geophys. Res.* 108.
- Skamarock, W., Klemp, J., Dudhia, J., Gill, D., Barker, D., Wang, W., Powers, J., 2007. A description of the advanced research wrf version 2. NCAR Technical Note, Boulder, Colorado, USA, NCAR/TN-468+STR.
- Tobias, A., Carnerero, C., Reche, C., Massagué, J., Via, M., Minguillon, M.C., Alastuey, A., Querol, X., 2020. Changes in air quality during the lockdown in Barcelona (Spain) one month into the SARS-CoV-2 epidemic. *Sci. Total Environ.* 726, 138540. <https://doi.org/10.1016/j.scitotenv.2020.138540>.
- Vautard, R., Beekmann, M., Menut, L., 2000. Applications of adjoint modelling in atmospheric chemistry: sensitivity and inverse modelling. *Environ. Model. Softw.* 15, 703–709.
- Vivanco, M., Bessagnet, B., Cuvelier, C., Theobald, M., Tsyro, S., Pirovano, G., Aulinger, A., Bieser, J., Calori, G., Ciarelli, G., Manders, A., Mircea, M., Aksoyoglu, S., Briganti, G., Cappelletti, A., Colette, A., Couvidat, F., D'Isidoro, M., Kranenburg, R., Meleux, F., Menut, L., Pay, M., Rouil, L., Silibello, C., Thunis, P., Ung, A., 2017. Joint analysis of deposition fluxes and atmospheric concentrations of inorganic nitrogen and sulphur compounds predicted by six chemistry transport models in the frame of the EURODELTAIII project. *Atmos. Environ.* 151, 152–175. <https://doi.org/10.1016/j.atmosenv.2016.11.042>.
- Von Storch, H., Langenberg, H., Feser, F., 2000. A spectral nudging technique for dynamical downscaling purposes. *Mon. Weather Rev.* 128, 3664–3673.
- Wilson, R.C., Fleming, Z.L., Monks, P.S., Clain, G., Henne, S., Konovalov, I.B., Szopa, S., Menut, L., 2012. Have primary emission reduction measures reduced ozone across Europe? An analysis of European rural background ozone trends 1996–2005. *Atmos. Chem. Phys.* 12, 437–454.